Computational Mechanics 26 (2000) 208–221 © Springer-Verlag 2000

Three-dimensional vibration of cylindrical shell panels – solution by continuum and discrete approaches

K. M. Liew, L. A. Bergman, T. Y. Ng, K. Y. Lam

Abstract This paper presents a three-dimensional elasticity solution to the free vibration problem of thick cylindrical shell panels of rectangular planform. The natural frequencies and corresponding mode shapes were obtained for thick cylindrical shell panels and detailed parametric investigations were carried out. Comparisons were also made with corresponding finite element simulation results. To validate the accuracy of the results as well as the stability of the present methodology, comprehensive convergence studies were also carried out. Further comparisons of present results were made with existing experimental and numerical results (classical, first-order and higher-order shell theories) available in open literature and the validity and range of applicability of the various shell theories examined.

1 Introduction

In view of the vast practical applications of shell structures which are many and varied such as aerospace, defence, marine and structural engineering, numerous studies in this area have been conducted over the years. In the 1950s, the popular use of cylindrical shells in the structural components of aircraft, missiles, submarines and rockets simulated many designers to optimize the shape of these structural components to best suit the particular application. Till today, the basic cylindrical shell structure has remained. One key area of interest is the development of simplified shell theories. Various forms of two-dimensional shell theories have been proposed to date. These range from the simplest classical thin shell hypothesis to the more complex shell theories which account for the higher-order effects of shear deformation and rotary inertia. The classical thin shell theory first postulated by Love (1888, 1927) for the analyses of thin elastic shells is similar to the Kirchoff–Love hypothesis for thin plates in that Love's first approximation for thin shells assumes a state of plane stress and inextensible normals that remain straight and normal during deformation. For thin shells, however, further approximations on the curvatures should be considered. On the basis of this general thin shell theory, different two-dimensional shell models have evolved over the years. These have been developed with the purpose of providing better descriptions of the physical phenomena of vibrating shells. Comprehensive reviews on the various derivations and applications of various thin shell theories have been reported by Leissa (1973).

Apart from solutions based on two-dimensional refined theories, formulations have been developed directly from the three-dimensional governing equation of linear elasticity. Such publications however remain relatively few in the literature. The first of such publications was by Armenakas et al. (1969) who presented substantial frequency results for an infinitely long isotropic hollow cylinder solved on the basis of a linear, three-dimensional theory of elasticity. This was followed by the frequency equations presented by Leissa (1973) for the vibration of closed circular cylindrical shells. Soldatos and Hadjigeorgiou (1990) proposed a semi-analytical three-dimensional approach for the free vibration analysis of cylindrical shell panels. A three-dimensional displacement field was assumed and the displacement components in the thickness direction were expanded in terms of a power series. Numerical results were presented for simply-supported cylindrical shell panels of various linear properties. The free vibration analysis of thick shells of revolution based on general three-dimensional displacement fields has also been reported by So (1993). A *p*-Ritz three-dimensional procedure was recently developed for the free vibration analysis of a class of solids with and without cavities (Hung et al. 1995; Liew and Hung 1995; Liew et al. 1995a, b).

The above are all global or continuum solution techniques. Several discrete techniques have been developed from the thin shell theories for the vibration study of shell panels. Reviews on progress in this research area have been reported notably by Qatu (1989) and more recently by Liew et al. (1997). At the forefront of the discretization approach is the finite element method which has been used extensively by many researchers to tackle various shell vibration problems. Deb Nath (1969) employed the

K. M. Liew (✉)
Centre for Advanced Numerical Engineering Simulations,
School of Mechanical and Production Engineering,
Nanyang Technological University, Singapore 639798

L. A. Bergman
Department of Aeronautical and Astronautical Engineering,
University of Illinois at Urbana-Champaign, Urbana,
IL 61801-2935, USA

T. Y. Ng, K. Y. Lam
Institute of High Performance Computing,
National University of Singapore,
89B Science Park Drive, #01-05/08, The Rutherford,
Singapore Science Park 1, Singapore 118261

rectangular finite elements to study the free vibration frequencies and mode shapes of fully clamped aluminium cylindrical shell panels. The computational results were validated with the experimentally determined vibration frequencies. Further finite element solutions to the free vibration problem of cylindrical shells were reported by Olson and Lindberg (1969) based on the singly-curved cylindrical shell finite elements. In their subsequent investigations, Olson and Lindberg (1971) used the doubly-curved triangular shell element to probe into the dynamic characteristics of both singly-curved cylindrical shell panels and doubly-curved spherical shell panels.

In this paper, the three-dimensional Ritz method is extended to the vibration study of thick cylindrical shell panels and detailed parametric investigations are carried out. Results obtained are compared with corresponding finite element simulation results using MSC/NASTRAN. Comprehensive convergence studies are also carried out to validate the accuracy of the results as well as the stability of the present methodology. Further comparisons of present results are also made with existing experimental and numerical results available in open literature. The validity and range of applicability of the existing classical, first-order and higher-order shell theories are commented.

2
Theory and formulation

2.1
Problem definition

Consider a homogeneous, isotropic, cylindrical shell panel of length a, width b, and thickness h, as shown in Fig. 1. The displacement components of the cylindrical shell panel are defined in a cylindrical co-ordinate system (r, θ, z). At the mid-surface, a chordwise principle radius of curvature R_m is defined. The subtended angle γ is related to the width a, and radius R_m of the cylindrical shell by

$$\gamma = 2\,\sin^{-1}\left(\frac{a}{2R_m}\right) \tag{1}$$

The top and bottom surfaces of the cylindrical shell panel are assumed to be free from stresses. At a general point within the shell domain, the displacement is resolved into u_1, u_2 and u_3 in the radial, circumferential and longitudinal directions with respect to the polar cylindrical reference frame. The boundary conditions of the edges are either free (F), freely supported (S) or clamped (C). The freely supported (S) boundary condition constrains the transverse deflection and the in-plane deflection tangential to the edge. The in-plane deflection normal to the edge, on the other hand, is set free. This study covers cylindrical shell panels with cantilevered (*CFFF*), freely supported (*SSSS*) and fully clamped (*CCCC*) boundary considered. For the cantilevered case, it is required that the three displacement components are constrained at the clamped edge ($z = 0$). The vibration characteristics of these cylindrical shell panels are to be determined.

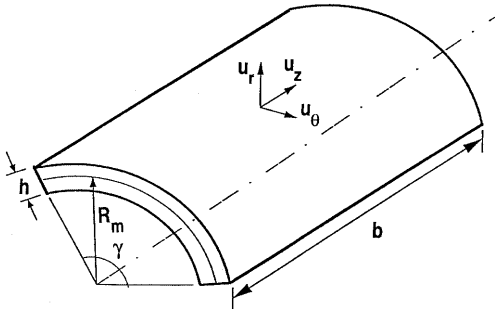

Fig. 1. Geometry and dimensions of a cylindrical shell panel

2.2
Method of solution

The linear elastic strain energy component $\hat{V}$ for a shell panel in a cylindrical co-ordinate system can be written in an integral form as

$$\hat{V} = \hat{\mathrm{E}} \int_{r_i}^{r_o} \int_{-\gamma/2}^{\gamma/2} \int_{-b/2}^{b/2} [(1-v)\tilde{\varepsilon}_1 + 2v\tilde{\varepsilon}_2 + (1-2v)\tilde{\varepsilon}_3] r\,\mathrm{d}r\,\mathrm{d}\theta\,\mathrm{d}z \tag{2}$$

where

$$\hat{\mathrm{E}} = \frac{E}{2(1+v)(1-2v)} \tag{3}$$

$$\tilde{\varepsilon}_1 = \varepsilon_{rr}^2 + \varepsilon_{\theta\theta}^2 + \varepsilon_{zz}^2 \tag{4}$$

$$\tilde{\varepsilon}_2 = \varepsilon_{rr}\varepsilon_{zz} + \varepsilon_{rr}\varepsilon_{\theta\theta} + \varepsilon_{\theta\theta}\varepsilon_{zz} \tag{5}$$

$$\tilde{\varepsilon}_3 = \varepsilon_{r\theta}^2 + \varepsilon_{rz}^2 + \varepsilon_{\theta z}^2 \tag{6}$$

and E is Young's modulus, v is Poisson's ratio, and the strain components in cylindrical polar co-ordinate for small deformation are given as

$$\varepsilon_{rr} = \frac{\partial u_1}{\partial r} \tag{7}$$

$$\varepsilon_{\theta\theta} = \frac{u_1}{r} + \frac{\partial u_2}{r\,\mathrm{d}\theta} \tag{8}$$

$$\varepsilon_{zz} = \frac{\partial u_3}{\partial z} \tag{9}$$

$$\varepsilon_{r\theta} = \frac{\partial u_1}{r\,\mathrm{d}\theta} + \frac{\partial u_2}{\partial r} - \frac{u_2}{r} \tag{10}$$

$$\varepsilon_{rz} = \frac{\partial u_1}{\partial z} + \frac{\partial u_3}{\partial r} \tag{11}$$

$$\varepsilon_{\theta z} = \frac{\partial u_2}{\partial z} + \frac{\partial u_3}{r\,\mathrm{d}\theta} \tag{12}$$

For free vibration analysis, the kinetic energy $\hat{T}$ can be expressed as

$$\hat{T} = \hat{\rho} \int_{r_i}^{r_o} \int_{-\gamma/2}^{\gamma/2} \int_{-b/2}^{b/2} \left[\dot{u}_1^2 + \dot{u}_2^2 + \dot{u}_3^2\right] r\,\mathrm{d}r\,\mathrm{d}\theta\,\mathrm{d}z \tag{13}$$

$$\dot{u}_1 = \frac{\partial u_1}{\partial t}; \quad \dot{u}_2 = \frac{\partial u_2}{\partial t}; \quad \dot{u}_3 = \frac{\partial u_3}{\partial t}; \quad \hat{\rho} = \frac{\rho}{2} \tag{14}$$

where ρ is the mass density, and t is time.

For linear, small-strain, simple harmonic motion, the displacement components assume the following forms

$$u_\alpha(r,\theta,z,t) = U_\alpha(r,\theta,z)\mathrm{e}^{\mathrm{i}\omega t}; \quad \alpha = 1,\ 2,\ 3 \tag{15}$$

where ω denotes the frequency of vibration and U_α the non-dimensional displacement amplitude functions.

For generality and simplicity in the subsequent derivations, the cylindrical co-ordinates (r,θ,z) are transformed into a set of non-dimensional parameters $(\bar{x}_1,\bar{x}_2,\bar{x}_3)$ by the following relations

$$r = \tfrac{1}{2}\left[(r_o + r_i) + (r_o - r)_i\bar{x}_1\right] \tag{16}$$

$$\theta = \hat{\gamma}\bar{x}_2 \tag{17}$$

$$z = \hat{b}\bar{x}_3 \tag{18}$$

in which $\hat{\gamma} = \gamma/2$ and $\hat{b} = b/2$.

The non-dimensional displacement amplitude functions are approximated by sets of one-dimensional functions $\psi_n^\alpha(\bar{x}_1)$ in the radial direction, and two-dimensional functions $\phi_m^\alpha(\bar{x}_2,\bar{x}_3)$ in the circumferential and chordwise directions in the form

$$U_\alpha(\bar{x}_1,\bar{x}_2,\bar{x}_3) = \sum_{m=1}^{M}\sum_{n=1}^{N} C_{mn}^\alpha \phi_m^\alpha(\bar{x}_2,\ \bar{x}_3)\psi_n^\alpha(\bar{x}_1) \tag{19}$$

in which $\langle\alpha = 1,\ 2,\ 3\rangle$, and C_{mn}^α are the unknown coefficients.

Let $\hat{\Pi}$ be the energy functional given by

$$\hat{\Pi} = \tilde{V} - \tilde{T} \tag{20}$$

where $\tilde{V}$ and $\tilde{T}$ are the maximum strain and kinetic energies of the plate which are derived by substituting Eq. (19) into the respective energy expressions in Eqs. (2) and (13) with the periodic component eliminated.

The minimisation of the functional in Eq. (20) with respect to the coefficients

$$\frac{\partial\hat{\Pi}}{\partial C_{mn}^\alpha} = 0; \quad \alpha = 1,\ 2,\ 3 \tag{21}$$

leads to the governing eigenvalue equation of the form

$$\left(\hat{\mathbf{K}} - \hat{\lambda}^2\hat{\mathbf{M}}\right)\hat{\mathbf{C}} = \mathbf{0} \tag{22}$$

where

$$\hat{\mathbf{K}} = \begin{bmatrix} \hat{\mathbf{k}}^{11} & \hat{\mathbf{k}}^{12} & \hat{\mathbf{k}}^{12} \\ & \hat{\mathbf{k}}^{22} & \hat{\mathbf{k}}^{23} \\ \text{Sym} & & \hat{\mathbf{k}}^{33} \end{bmatrix} \tag{23}$$

$$\hat{\mathbf{M}} = \begin{bmatrix} \hat{\mathbf{m}}^{11} & 0 & 0 \\ & \hat{\mathbf{m}}^{22} & 0 \\ \text{Sym} & & \hat{\mathbf{m}}^{33} \end{bmatrix} \tag{24}$$

and

$$\hat{\mathbf{C}} = \left\{\ \mathbf{C}^1 \quad \mathbf{C}^2 \quad \mathbf{C}^3\ \right\}^{\mathrm{T}} \tag{25}$$

The explicit form of the respective elements in the stiffness submatrices $\hat{\mathbf{k}}^{\alpha\beta}$ are given by:

$$\begin{aligned}\hat{\mathrm{k}}_{mjnk}^{11} = {} & \frac{(1-\nu)R_m^2}{\tilde{\Lambda}_1}\left[\frac{4}{h^2}\left(\hat{\mathbf{I}}_{mj}^{0000}\right)_{11}\left(\hat{\mathbf{J}}_{nk}^{11;1}\right)_{11} + \left(\hat{\mathbf{I}}_{mj}^{0000}\right)_{11}\left(\hat{\mathbf{J}}_{nk}^{00;-1}\right)_{11}\right] \\ & + \frac{2\nu R_m^2}{\tilde{\Lambda}_1 h}\left[\left(\hat{\mathbf{I}}_{mj}^{0000}\right)_{11}\left(\hat{\mathbf{J}}_{nk}^{01;0}\right)_{11} + \left(\hat{\mathbf{I}}_{mj}^{0000}\right)_{11}\left(\hat{\mathbf{J}}_{nk}^{10;0}\right)_{11}\right] \\ & + \frac{4R_m^2}{\tilde{\Lambda}_2}\left[\frac{1}{b^2}\left(\hat{\mathbf{I}}_{mj}^{0101}\right)_{11}\left(\hat{\mathbf{J}}_{nk}^{00;1}\right)_{11} + \frac{1}{\gamma^2}\left(\hat{\mathbf{I}}_{mj}^{1010}\right)_{11}\left(\hat{\mathbf{J}}_{nk}^{00;-1}\right)_{11}\right]\end{aligned} \tag{26}$$

$$\begin{aligned}\hat{\mathrm{k}}_{mjnk}^{12} = {} & \frac{2(1-\nu)R_m^2}{\tilde{\Lambda}_1\gamma}\left[\left(\hat{\mathbf{I}}_{mj}^{0010}\right)_{12}\left(\hat{\mathbf{J}}_{nk}^{00;-1}\right)_{12} + \frac{2\nu R_m^2}{\tilde{\Lambda}_1 h}\left(\hat{\mathbf{I}}_{mj}^{0010}\right)_{12}\left(\hat{\mathbf{J}}_{nk}^{10;0}\right)_{12}\right] \\ & + \frac{2R_m^2}{\tilde{\Lambda}_2\gamma}\left[\frac{2}{h}\left(\hat{\mathbf{I}}_{mj}^{1000}\right)_{12}\left(\hat{\mathbf{J}}_{nk}^{01;0}\right)_{12} - \left(\hat{\mathbf{I}}_{mj}^{1000}\right)_{12}\left(\hat{\mathbf{J}}_{nk}^{00;-1}\right)_{12}\right]\end{aligned} \tag{27}$$

$$\begin{aligned}\hat{\mathrm{k}}_{mjnk}^{13} = {} & \frac{2\nu R_m^2}{\tilde{\Lambda}_1 h}\left[\frac{2}{b}\left(\hat{\mathbf{I}}_{mj}^{0001}\right)_{13}\left(\hat{\mathbf{J}}_{nk}^{10;1}\right)_{13} + \left(\hat{\mathbf{I}}_{mj}^{0001}\right)_{13}\left(\hat{\mathbf{J}}_{nk}^{00;0}\right)_{13}\right] \\ & + \frac{4R_m^2}{\tilde{\Lambda}_2 hb}\left(\hat{\mathbf{I}}_{mj}^{0100}\right)_{13}\left(\hat{\mathbf{J}}_{nk}^{01;1}\right)_{13}\end{aligned} \tag{28}$$

$$\begin{aligned}\hat{\mathrm{k}}_{mjnk}^{22} = {} & \frac{(1-\nu)R_m^2}{\tilde{\Lambda}_1\gamma^2}\left(\hat{\mathbf{I}}_{mj}^{1010}\right)_{22}\left(\hat{\mathbf{J}}_{nk}^{00;-1}\right)_{22} \\ & + \frac{4R_m^2}{\tilde{\Lambda}_2}\left[\frac{1}{h^2}\left(\hat{\mathbf{I}}_{mj}^{0000}\right)_{22}\left(\hat{\mathbf{J}}_{nk}^{11;1}\right)_{22} + \frac{1}{b^2}\left(\hat{\mathbf{I}}_{mj}^{0101}\right)_{22}\left(\hat{\mathbf{J}}_{nk}^{00;1}\right)_{22}\right] \\ & + \frac{R_m^2}{\tilde{\Lambda}_2}\left(\hat{\mathbf{I}}_{mj}^{0000}\right)_{22}\left(\hat{\mathbf{J}}_{nk}^{00;-1}\right)_{22} \\ & + \frac{2R_m^2}{\tilde{\Lambda}_2 h}\left[\left(\hat{\mathbf{I}}_{mj}^{0000}\right)_{22}\left(\hat{\mathbf{J}}_{nk}^{01;0}\right)_{22} + \left(\hat{\mathbf{I}}_{mj}^{0000}\right)_{22}\left(\hat{\mathbf{J}}_{nk}^{10;0}\right)_{22}\right]\end{aligned} \tag{29}$$

$$\begin{aligned}\hat{\mathrm{k}}_{mjnk}^{23} = {} & \frac{4R_m^2}{b\gamma}\left[\frac{\nu}{\tilde{\Lambda}_1}\left(\hat{\mathbf{I}}_{mj}^{1001}\right)_{23}\left(\hat{\mathbf{J}}_{nk}^{00;0}\right)_{23} + \frac{1}{\tilde{\Lambda}_2}\left(\hat{\mathbf{I}}_{mj}^{0110}\right)_{23}\left(\hat{\mathbf{J}}_{nk}^{00;0}\right)_{23}\right]\end{aligned} \tag{30}$$

$$\begin{aligned}\hat{\mathrm{k}}_{mjnk}^{33} = {} & \frac{(1-\nu)R_m^2}{\tilde{\Lambda}_1 b^2}\left(\hat{\mathbf{I}}_{mj}^{0101}\right)_{33}\left(\hat{\mathbf{J}}_{nk}^{00;1}\right)_{33} \\ & + \frac{R_m^2}{\tilde{\Lambda}_2}\left[\frac{4}{h^2}\left(\hat{\mathbf{I}}_{mj}^{0000}\right)_{33}\left(\hat{\mathbf{J}}_{nk}^{11;1}\right)_{33} + \frac{1}{\gamma^2}\left(\hat{\mathbf{I}}_{mj}^{1010}\right)_{33}\left(\hat{\mathbf{J}}_{nk}^{00;-1}\right)_{33}\right]\end{aligned} \tag{31}$$

and the elements in the mass submatrix $\hat{\mathbf{m}}^{\alpha\beta}$ are given by

$$\hat{\mathrm{m}}^{11}_{mjnk} = \left(\hat{\mathbf{I}}^{0000}_{mj}\right)_{11}\left(\hat{\mathbf{J}}^{00;1}_{nk}\right)_{11} \tag{32}$$

$$\hat{\mathrm{m}}^{22}_{mjnk} = \left(\hat{\mathbf{I}}^{0000}_{mj}\right)_{22}\left(\hat{\mathbf{J}}^{00;1}_{nk}\right)_{22} \tag{33}$$

$$\hat{\mathrm{m}}^{33}_{mjnk} = \left(\hat{\mathbf{I}}^{0000}_{mj}\right)_{33}\left(\hat{\mathbf{J}}^{00;1}_{nk}\right)_{33} \tag{34}$$

where

$$\tilde{\Lambda}_1 = \tfrac{1}{2}(1-2\nu)\tilde{\Lambda}_2 \tag{35}$$

$$\tilde{\Lambda}_2 = 2(1+\nu) \tag{36}$$

and

$$\left(\hat{\mathbf{I}}^{defg}_{mj}\right)_{\alpha\beta} = \int_{-1}^{1}\int_{-1}^{1}\left[\frac{\partial^{d+e}\phi^{\alpha}_{m}(\bar{x}_2,\bar{x}_3)}{\partial x_2^{d}\,\partial x_3^{e}}\right] \times \left[\frac{\partial^{f+g}\phi^{\beta}_{j}(\bar{x}_2,\bar{x}_3)}{\partial x_2^{f}\partial x_3^{g}}\right]\mathrm{d}\bar{x}_2\,\mathrm{d}\bar{x}_3 \tag{37}$$

$$\left(\hat{\mathbf{J}}^{rs;\,Z}_{nk}\right)_{\alpha\beta} = \int_{-1}^{1}\left[\frac{\partial^{r}\psi^{\alpha}_{n}(\bar{x}_1)}{\partial x_1^{r}}\right]\left[\frac{\partial^{s}\psi^{\beta}_{k}(\bar{x}_1)}{\partial x_1^{s}}\right]\hat{\vartheta}(\bar{x}_1)\mathrm{d}\bar{x}_1 \tag{38}$$

$$\hat{\vartheta}(\bar{x}_1) = \tfrac{1}{2}\left[(r_o+r_i)+(r_o-r_i)\bar{x}_1\right] \tag{39}$$

in which $\langle(\alpha);\ (\beta)=(1,2,3);\ (1,2,3)\rangle$.

The eigenvalues obtained from Eq. (22) are given by

$$\hat{\lambda} = \omega R_m\sqrt{\frac{\rho}{E}} \tag{40}$$

which is redefined in terms of non-dimensionalized frequency parameter λ of the following form that is independent of h:

$$\lambda = \frac{a}{R_m}\hat{\lambda} = \omega a\sqrt{\frac{\rho}{E}} \tag{41}$$

2.3 Admissible displacement functions

The admissible functions adopted in Eq. (19) are sets of one $\psi^{\alpha}_{n}(\bar{x}_3)$ and two-dimensional $\phi^{\alpha}_{m}(\bar{x}_1,\bar{x}_2)$ orthogonal polynomial functions. Details of these orthogonal polynomial functions have been given earlier by Liew et al. (1995). To be able to use the procedures given by Liew et al. (1995), one needs to know the basic functions which are defined by the boundary conditions of the cylindrical shell panels. In this study, we consider only the shell panels with *CFFF*, *SSSS* and *CCCC* boundary conditions.

The one-dimensional polynomial functions $\psi^{\alpha}_{n}(\bar{x}_1)$ approximate the displacement variations in the thickness direction of the cylindrical shell. These functions are constructed to satisfy the boundary conditions of the shell at the top and bottom surfaces ($r = r_i$ and r_o). Since the top and bottom surfaces of the shell panel are assumed to be free from stresses, the following one-dimensional basic functions are chosen for the present analysis

$$\psi^{\alpha}_{1}(\bar{x}_1) = 1 \tag{42}$$

in which $\langle\alpha = 1,\ 2,\ 3\rangle$.

The two-dimensional functions $\phi^{\alpha}_{m}(\bar{x}_2,\bar{x}_3)$ approximate the displacement variations of the shell panel in both the spanwise and chordwise directions. The general forms of the functions are:

- *CFFF* shell panels

$$\phi^{\alpha}_{1}(\bar{x}_2,\bar{x}_3) = (\bar{x}_3+1);\quad \alpha = 1,\ 2,\ 3 \tag{43}$$

- *SSSS* shell panels

$$\phi^{\alpha}_{1}(\bar{x}_2,\bar{x}_3) = (\bar{x}_2^2-1)^{\hat{\Theta}^{\alpha}_{1}}(\bar{x}_3^2-1)^{\hat{\Theta}^{\alpha}_{2}} \tag{44}$$

$$\alpha = \begin{cases} 1; & \hat{\Theta}^1_1 = \hat{\Theta}^1_1 = 1 \\ 2; & \hat{\Theta}^2_1 = 0 \text{ and } \hat{\Theta}^2_1 = 1 \\ 3; & \hat{\Theta}^3_1 = 1 \text{ and } \hat{\Theta}^3_1 = 0 \end{cases} \tag{45}$$

- *CCCC* shell panels

$$\phi^{\alpha}_{1}(\bar{x}_2,\bar{x}_3) = (\bar{x}_2^2-1)(\bar{x}_3^2-1);\quad \alpha = 1,\ 2,\ 3 \tag{46}$$

Apart from satisfying the boundary conditions of the cylindrical shell panels, the two-dimensional polynomials also account for the symmetry classes of the vibration modes. For the *CFFF* shell, the vibration modes can be divided into symmetry (S) and antisymmetry (A) modes with respect to the $\bar{x}_1\bar{x}_2$ plane. For the *SSSS* and *CCCC* shell panels, the vibration modes are divided into four distinct families of symmetry classes. These are the doubly symmetry (SS), symmetry antisymmetry (SA), antisymmetry symmetry (AS) and doubly antisymmetry (AA) modes. The symmetry consideration are accounted for in the choice of the two-dimensional generating functions. Details of the functions are given in Liew et al. (1995).

3 Results and discussion

3.1 Convergence studies

The reliability and accuracy of the frequency parameters obtained in this study are established through convergence tests and comparison studies. Table 1 shows the improvement on the frequency parameters λ, for the cantilevered cylindrical shell at different solution sizes. The rate of convergence of the frequency parameters for the cylindrical shells with *SSSS* and *CCCC* boundary conditions are examined in Table 2. Through these convergence tests, the optimum number of terms required in the present formulation for reliable solutions can be determined. For the *CFFF* shells, the aspect ratios (b/a) are fixed at 1 and 3 for the convergence test. The thickness ratios (h/a) are taken as 0.1 (moderately thick) and 0.5 (thick). The shallowness ratio for all the cases considered in the convergence study is fixed at $a/R_m = 0.5$ which corresponds to a fairly shallow shell.

It is observed in Table 1 that the eigenvalues converge monotonically downwards towards the exact value as higher number of terms are assumed in the polynomial shape functions. The number of terms N, for the one-dimensional thickness function and the degree of

Table 1. Convergence of frequency parameters $\lambda = \omega a\sqrt{\rho/E}$ for a cantilevered cylindrical shell of rectangular planform (radius of curvature $a/R_m = 0.5$)

Thickness ratio h/a	No. of terms P, N	Symmetry classes and mode sequence number							
		S-1	S-2	S-3	S-4	A-1	A-2	A-3	A-4
(a) Cylindrical shell of square planform ($b/a = 1$)									
0.01	$P = 5, N = 3$	0.053564	0.095578	0.19601	0.35014	0.033414	0.17543	0.20600	0.36828
	$P = 6, N = 4$	0.052372	0.092382	0.14514	0.27838	0.032374	0.12957	0.19453	0.27848
	$P = 7, N = 5$	0.052178	0.091978	0.14512	0.27362	0.032235	0.12871	0.19401	0.27214
	$P = 7, N = 6$	0.052177	0.091978	0.14411	0.27361	0.032235	0.12870	0.19398	0.27212
	$P = 8, N = 5$	0.052131	0.091925	0.14400	0.27338	0.032200	0.12858	0.19397	0.27187
	$P = 9, N = 5$	0.052084	0.091863	0.14390	0.27314	0.032167	0.12848	0.19395	0.27167
	$P = 10, N = 5$	0.052071	0.091858	0.14383	0.27308	0.032157	0.12841	0.19394	0.27155
0.5	$P = 5, N = 3$	0.45004	1.6030	1.7482	2.2544	0.67581	0.79013	1.8048	2.3002
	$P = 5, N = 5$	0.44359	1.5932	1.6535	2.2406	0.66905	0.78273	1.7731	2.2004
	$P = 6, N = 5$	0.44359	1.5930	1.6532	2.2405	0.66904	0.78273	1.7729	2.2000
	$P = 5, N = 6$	0.44319	1.5924	1.6524	2.2402	0.66865	0.78245	1.7727	2.1994
	$P = 5, N = 7$	0.44296	1.5921	1.6520	2.2402	0.65844	0.78230	1.7727	2.1991
	$P = 5, N = 8$	0.44281	1.5919	1.6518	2.2401	0.66832	0.78221	1.7727	2.1989
	$P = 5, N = 9$	0.44271	1.5918	1.6516	2.2401	0.66825	0.78215	1.7726	2.1988
(b) Cylindrical shell of rectangular planform ($b/a = 3$)									
0.5	$P = 5, N = 3$	0.17201	0.98754	1.6012	2.3514	0.32787	0.75642	1.6120	2.4767
	$P = 5, N = 5$	0.16805	0.94077	1.5839	2.3242	0.32109	0.74511	1.4538	2.2436
	$P = 6, N = 5$	0.16805	0.94053	1.5836	2.3240	0.32188	0.74496	1.4537	2.2434
	$P = 5, N = 6$	0.16770	0.93918	1.5826	2.3079	0.31956	0.74439	1.4523	2.2409
	$P = 5, N = 7$	0.16751	0.93828	1.5818	2.3064	0.31926	0.74403	1.4515	2.2398
	$P = 5, N = 8$	0.16733	0.93744	1.5814	2.3046	0.31905	0.74382	1.4507	2.2388
	$P = 5, N = 9$	0.16731	0.93735	1.5812	2.3044	0.31893	0.74370	1.4507	2.2388

Table 2. Convergence of frequency parameters $\lambda = \omega a\sqrt{\rho/E}$ for a cantilevered cylindrical shell of rectangular planform subject to different boundary conditions (radius of curvature $a/R_m = 0.5$)

Thickness ratio h/a	No. of terms P, N	Symmetry classes and mode sequence number											
		SS-1	SS-2	SS-3	SA-1	SA-2	SA-3	AS-1	AS-2	AS-3	AA-1	AA-2	AA-3
(a) Cylindrical shell with simply-supported edges (*SSSS*)													
0.2	$P = 5, N = 4$	1.0556	2.7596	3.9297	1.9283	2.3396	4.3556	1.9483	2.2804	4.3283	3.3412	3.8559	3.8967
	$P = 6, N = 4$	1.0556	2.7596	3.9297	1.9283	2.3396	4.3556	1.9483	2.2804	4.3283	3.3412	3.8559	3.8967
	$P = 5, N = 6$	1.0555	2.7596	3.9242	1.9283	2.3385	4.3556	1.9483	2.2791	4.3283	3.3378	3.8559	3.8967
	$P = 5, N = 7$	1.0555	2.7596	3.9242	1.9283	2.3385	4.3556	1.9483	2.2791	4.3283	3.3378	3.8559	3.8967
	$P = 5, N = 8$	1.0555	2.7596	3.9242	1.9283	2.3385	4.3556	1.9483	2.2791	4.3283	3.3378	3.8559	3.8967
	$P = 5, N = 9$	1.0555	2.7596	3.9242	1.9283	2.3385	4.3556	1.9483	2.2791	4.3283	3.3378	3.8559	3.8967
0.5	$P = 5, N = 4$	1.8397	2.7626	4.3082	1.9278	3.4838	4.3581	1.9483	3.4312	4.3063	3.8276	3.8967	4.6159
	$P = 6, N = 4$	1.8397	2.7626	4.3082	1.9278	3.4838	4.3581	1.9483	3.4312	4.3063	3.8276	3.8967	4.6159
	$P = 5, N = 6$	1.8361	2.7626	4.3067	1.9278	3.4651	4.3579	1.9483	3.4121	4.3060	3.8276	3.8967	4.5771
	$P = 5, N = 7$	1.8361	2.7626	4.3067	1.9278	3.4650	4.3579	1.9483	3.4121	4.3060	3.8276	3.8967	4.5769
	$P = 5, N = 8$	1.8361	2.7626	4.3067	1.9278	3.4650	4.3579	1.9483	3.4121	4.3060	3.8276	3.8967	4.5769
	$P = 5, N = 9$	1.8361	2.7626	4.3067	1.9278	3.4650	4.3579	1.9483	3.4121	4.3060	3.8276	3.8967	4.5769
(b) Cylindrical shell with fully clamped edges (*CCCC*)													
0.2	$P = 5, N = 4$	1.6744	4.3468	4.4461	2.8805	3.7386	5.1572	2.7993	3.7484	5.1958	3.8082	4.4358	5.4292
	$P = 6, N = 4$	1.6744	4.3467	4.4461	2.8804	3.7385	5.1572	2.7993	3.7482	5.1957	3.8082	4.4357	5.4290
	$P = 5, N = 6$	1.6708	4.3307	4.4294	2.8721	3.7373	5.1369	2.7911	3.7469	5.1754	3.7959	4.4354	5.4272
	$P = 5, N = 7$	1.6707	4.3305	4.4291	2.8718	3.7370	5.1367	2.7908	3.7466	5.1751	3.7955	4.4353	5.4269
	$P = 5, N = 8$	1.6705	4.3299	4.4285	2.8716	3.7370	5.1361	2.7906	3.7466	5.1746	3.7952	4.4353	5.4268
	P = 5, $N = 9$	1.6705	4.3299	4.4285	2.8715	3.7370	5.1361	2.7905	3.7466	5.1745	3.7952	4.4353	5.4268
0.5	$P = 5, N = 4$	2.3636	5.3178	5.4495	3.6838	3.7550	5.4930	3.5209	3.8014	5.5594	4.3750	4.8139	5.3730
	$P = 6, N = 4$	2.3636	5.3178	5.4495	3.6838	3.7550	5.4930	3.5209	3.8014	5.5594	4.3750	4.8139	5.3730
	$P = 5, N = 6$	2.3460	5.2682	5.3947	3.6569	3.7492	5.4708	3.5017	3.7882	5.5378	4.3715	4.7741	5.3627
	$P = 5, N = 7$	2.3448	5.2658	5.3919	3.6553	3.7483	5.4703	3.5004	3.7870	5.5373	4.3713	4.7720	5.3611
	$P = 5, N = 8$	2.3440	5.2643	5.3903	3.6544	3.7480	5.4700	3.4996	3.7865	5.5370	4.3712	4.7708	5.3606
	$P = 5, N = 9$	2.3438	5.2640	5.3900	3.6541	3.7476	5.4699	3.4994	3.7862	5.5369	4.3711	4.7706	5.3601

polynomials P, for the two-dimensional surface functions are increased steadily to achieve converged solutions. The natural frequencies of the *CFFF* shells are presented in two symmetry classes. It is observed that for the *CFFF* shell, the computed frequency parameters improve with higher order terms being assumed in the two-dimensional functions. Comparatively, the influence of the number of terms N, of the one-dimensional polynomial functions on the rate of convergence of the eigenvalues is less significant. It is established that reliable frequency parameters for a thin ($h/a = 0.01$) cantilevered shell can be obtained with two-dimensional functions of polynomial order $P = 10$ and one-dimensional functions of total number of terms $N = 5$. As the shell thickness increases, reasonably converged solutions are obtained at $P = 5$ and $N = 9$.

For the cases considered in Table 2, the shells possess four symmetry classes of vibration and thus the number of terms needed in the deflection functions for converged solutions are relatively fewer than that for the *CFFF* shells (which have only two types of symmetry modes). It is observed that both the *SSSS* and *CCCC* cylindrical shells require the same number of terms for converged solutions. To ensure that the frequency solutions used in the subsequent discussion are sufficiently accurate, appropriate number of terms of the one- and two- dimensional polynomial functions are employed in the solution process.

Further, present three-dimensional convergence characteristics are compared with FEM results generated by the commercial software MSC/NASTRAN using 8-noded solid elements. The results are presented in Table 3 for shell panels of square planform with thickness ratio $h/a = 0.5$ and shallowness ratio $a/R_m = 0.5$. The *CFFF*, *SSSS* and *CCCC* boundary conditions were all considered. The FEM results display reasonably well converged results when using a $50 \times 50 \times 10$ grid size or 25,000 elements. It is also observed that the present three-dimensional elasticity solutions agree very well with the FEM results generated by MSC/NASTRAN for all the three boundary condition cases with less than 1% difference between the two sets of results.

Table 3. Convergence of frequency parameters $\lambda = \omega a\sqrt{\rho/E}$ for a cantilevered cylindrical shell of square planform by three-dimensional elasticity theory and FEM using MSC/NASTRAN (radius of curvature $a/R_m = 0.5$, thickness ratio $h/a = 0.5$)

Solution method	No. of terms and grid size	Symmetry classes and mode sequence number											
		S-1	S-2	S-3	S-4	A-1	A-2	A-3	A-4				
(a) Cantilevered cylindrical shell (*CFFF*)													
	$P = 5, N = 3$	0.45004	1.6030	1.7482	2.2544	0.67581	0.79013	1.8048	2.3002				
	$P = 5, N = 5$	0.44359	1.5932	1.6535	2.2406	0.66905	0.78273	1.7731	2.2004				
Present 3-D	$P = 6, N = 5$	0.44359	1.5930	1.6532	2.2405	0.66904	0.78273	1.7729	2.2000				
	$P = 5, N = 6$	0.44319	1.5924	1.6524	2.2402	0.66865	0.78245	1.7727	2.1994				
	$P = 5, N = 7$	0.44296	1.5921	1.6520	2.2402	0.65844	0.78230	1.7727	2.1991				
	$P = 5, N = 8$	0.44281	1.5919	1.6518	2.2401	0.66832	0.78221	1.7727	2.1989				
	$P = 5, N = 9$	0.44271	1.5918	1.6516	2.2401	0.66825	0.78215	1.7726	2.1988				
FEM using MSC/ NASTRAN	$20 \times 20 \times 4$	0.44347	1.5945	1.6451	2.2438	0.6692	0.7836	1.7757	2.2025				
	$30 \times 30 \times 6$	0.44181	1.5885	1.6479	2.2354	0.6667	0.7807	1.7690	2.1945				
	$40 \times 40 \times 8$	0.44108	1.5859	1.6453	2.2318	0.6657	0.7794	1.7661	2.1909				
	$50 \times 50 \times 10$	0.44106	1.5858	1.6452	2.2317	0.6656	0.7794	1.7660	2.1908				
		SS-1	SS-2	SS-3	SA-1	SA-2	SA-3	AS-1	AS-2	AS-3	AA-1	AA-2	AA-3
(b) Cylindrical shell with simply-supported edges (*SSSS*)													
0.5	$P = 5, N = 4$	1.8397	2.7626	4.3082	1.9278	3.4838	4.3581	1.9483	3.4312	4.3063	3.8276	3.8967	4.6159
	$P = 6, N = 4$	1.8397	2.7626	4.3082	1.9278	3.4838	4.3581	1.9483	3.4312	4.3063	3.8276	3.8967	4.6159
	$P = 5, N = 6$	1.8361	2.7626	4.3067	1.9278	3.4651	4.3579	1.9483	3.4121	4.3060	3.8276	3.8967	4.5771
	$P = 5, N = 7$	1.8361	2.7626	4.3067	1.9278	3.4650	4.3579	1.9483	3.4121	4.3060	3.8276	3.8967	4.5769
	$P = 5, N = 8$	1.8361	2.7626	4.3067	1.9278	3.4650	4.3579	1.9483	3.4121	4.3060	3.8276	3.8967	4.5769
	$P = 5, N = 9$	1.8361	2.7626	4.3067	1.9278	3.4650	4.3579	1.9483	3.4121	4.3060	3.8276	3.8967	4.5769
FEM using MSC/ NASTRAN	$20 \times 20 \times 4$	1.8414	2.7706	4.3191	–	3.4751	4.3704	–	3.4219	4.3184	3.8386	3.9080	4.5901
	$30 \times 30 \times 6$	1.8347	2.7605	4.3034	–	3.4623	4.3545	–	3.4094	4.3028	3.8245	3.8937	4.5733
	$40 \times 40 \times 8$	1.8320	2.7566	4.2973	–	3.4574	4.3484	–	3.4046	4.2966	3.8193	3.8882	4.5669
	$50 \times 50 \times 10$	1.8320	2.7565	4.2971	–	3.4573	4.3482	–	3.4045	4.2964	3.8191	3.8880	4.5667
(c) Cylindrical shell with fully clamped edges (*CCCC*)													
0.5	$P = 5, N = 4$	2.3636	5.3178	5.4495	3.6838	3.7550	5.4930	3.5209	3.8014	5.5594	4.3750	4.8139	5.3730
	$P = 6, N = 4$	2.3636	5.3178	5.4495	3.6838	3.7550	5.4930	3.5209	3.8014	5.5594	4.3750	4.8139	5.3730
	$P = 5, N = 6$	2.3460	5.2682	5.3947	3.6569	3.7492	5.4708	3.5017	3.7882	5.5378	4.3715	4.7741	5.3627
	$P = 5, N = 7$	2.3448	5.2658	5.3919	3.6553	3.7483	5.4703	3.5004	3.7870	5.5373	4.3713	4.7720	5.3611
	$P = 5, N = 8$	2.3440	5.2643	5.3903	3.6544	3.7480	5.4700	3.4996	3.7865	5.5370	4.3712	4.7708	5.3606
	$P = 5, N = 9$	2.3438	5.2640	5.3900	3.6541	3.7476	5.4699	3.4994	3.7862	5.5369	4.3711	4.7706	5.3601
FEM using MSC/ NASTRAN	$20 \times 20 \times 4$	2.3474	5.2728	5.3990	3.6604	3.7537	5.4790	3.5055	3.7925	5.5463	4.3785	4.7787	5.3690
	$30 \times 30 \times 6$	2.3389	5.2530	5.3788	3.6466	3.7397	5.4585	3.4922	3.7783	5.5254	4.3621	4.7607	5.3489
	$40 \times 40 \times 8$	2.3351	5.2445	5.3701	3.6406	3.7337	5.4497	3.4866	3.7723	5.5166	4.3550	4.7530	5.3404
	$50 \times 50 \times 10$	2.3350	5.2443	5.3699	3.6405	3.7335	5.4495	3.4864	3.7721	5.5163	4.3548	4.7528	5.3402

3.2
Comparison studies

The reliability of the frequency results obtained in the present formulation for cylindrical shells is further established by comparing with existing experimental and numerical results available in the literature. For this purpose, a cantilevered (*CFFF*) steel fan blade of square planform with length $a = b = 12.0$ in., thickness $h = 0.120$ in. and radius $R_m = 24.0$ in. is considered. The *CFFF* steel fan blade has been experimentally tested by Olson and Lindberg (1971). The vibration frequencies are compared in Table 4 together with the finite element results, the classical thin plate solutions and the present three-dimensional elasticity solutions. In the present calculation, the standard material properties (E and ρ) of steel are assumed. The finite element results are extracted from the work of Olson and Lindberg (1969, 1971) and Walker (1978). The classical thin plate solutions, on the other hand, have been computed by Leissa et al. (1981) and Lim and Liew (1994) from the Rayleigh–Ritz method. From Table 4, it is observed that the present three-dimensional solutions are applicable for the analysis of thin shells and the results are in good agreement with the experimental results and analytical Kirchoff–Love thin shell solutions.

Further comparisons with the experimental results are carried out for a fully clamped (*CCCC*) aluminum cylindrical shell. The experimental and computational frequencies reported by Deb Nath (1969) for this specimen are listed together with the current predictions based on the three-dimensional Ritz method. Deb Nath (1969) computed the frequencies of the fully clamped shell using the rectangular finite element. Other numerical techniques have also been applied to this specimen. These include the triangular finite element approach proposed by Olson and Lindberg (1971), the spline finite strip method of Cheung et al. (1989) and the thin shell Rayleigh–Ritz method of Lim and Liew (1994) and Webster (1968). Table 5 summarizes the experimental natural frequencies and numerical predictions for the *CCCC* aluminum cylindrical shell from these different approaches. It is observed from Table 5 that the present three-dimensional frequency results correlate reasonably well with the reported finite element and analytical solutions which are derived from the thin shell theory. The experimental frequencies, however, tend to be lower than the analytical solutions. This is generally the case, since it is difficult to impose perfect clamping conditions experimentally especially for the fully clamped shell. This explains the discrepancy between the experimentally determined frequencies and the numerical predictions from both the classical thin shell theory and the present three-dimensional method.

Solutions from the refined shell theories and the present three-dimensional solutions are presented in Tables 6 and 7 for thick cantilevered and fully clamped cylindrical shells, respectively. The frequency solutions based on the

Table 4. Comparison of experimental frequencies (Hz) and analytical solutions for the cantilever cylindrical steel fan blade with $E = 210$ GPa, $\rho = 7860$ kg/m^3, $\nu = 0.3$, $R_m = 24.0$ in., $h = 0.120$ in. and $a = b = 12.0$ in

Source of results	Symmetry classes and mode sequence number									
	S-1	S-2	S-3	S-4	S-5	A-1	A-2	A-3	A-4	A-5
Experimental[a]	134.5	259	395	751	790	85.6	351	531	743	809
Finite element method[b]	139.17	251.30	393.42	746.37	790.10	86.601	348.59	533.37	752.09	813.84
Finite element method[c]	147.6	255.1	423.5	792.2	–	93.47	393.1	534.3	781.5	–
Walker (1978)	139.6	249.0	398.5	761.4	–	86.6	351.0	534.5	749.0	–
Leissa et al. (1981)	137.8	248.6	387.4	738.4	–	85.94	342.9	531.9	736.3	–
Lim and Liew (1994)	135.35	244.23	379.95	716.94	759.81	84.406	336.45	521.60	715.19	790.71
Present 3-D solutions	140.12	248.94	389.79	740.07	785.01	87.148	348.00	525.59	735.92	804.92

[a] Experimental results by Olsen and Lindberg (1971)
[b] Finite element solutions based on a doubly-curved triangular element by Olsen and Lindberg (1971)
[c] Finite element solutions based on a cylindrical shell element by Olsen and Lindberg (1969)

Table 5. Comparison of experimental frequencies (Hz) and analytical solutions for the fully clamped aluminium cylindrical shell with $E = 10^7$ lbf/in^2, $\rho = 0.096$ lb/in^2, $\nu = 0.33$, $R_m = 30.0$ in., $h = 0.013$ in., $a = 4.0$ and $b = 3.0$ in

Source of reference	Symmetry classes and mode sequence number											
	SS-1	SS-2	SS-3	SA-1	SA-2	SA-3	AS-1	AS-2	AS-3	AA-1	AA-2	AA-3
Olsen and Lindberg (1971) – Expt	940	1260	2100	1306	1802	–	814	1770	2225	1452	2280	–
Deb Nath (1969)	973	1311	2068	1371	1775	–	890	1816	2234	1454	2319	–
Webster (1968)	958	1288	2057	1364	1753	–	870	1795	2220	1440	2300	–
Olsen and Lindberg (1971) – FEM	958	1288	2056	1363	1756	–	870	1780	2222	1440	2295	–
Cheung et al. (1989)	963	1298	–	1369	–	–	874	–	–	–	–	–
Lim and Liew (1994)	958.22	1288.6	2056.4	1364.0	1753.7	–	870.10	1779.9	2218.9	1440.2	2289.2	–
Present 3-D solutions	960.26	1292.5	2058.9	1364.8	1761.1	3058.9	872.39	1786.8	2223.2	1443.0	2289.2	3285.3

Table 6. Comparison of frequency parameters $\lambda = \omega a\sqrt{\rho/E}$ for moderately thick cantilever cylindrical shells of square planform computed based on three-dimensional theory and approximate theories ($a/R_m = 0.5$, $h/a = 0.1$)

Source of results	Symmetry classes and mode sequence number							
	S-1	S-2	S-3	S-4	A-1	A-2	A-3	A-4
First-order theory[a]	0.11852	0.63618	0.77727	1.4405	0.24477	0.65826	0.85814	1.7292
Third-order theory[b]	0.11824	0.63703	0.77458	1.4438	0.24427	0.65843	0.85829	1.7265
Higher-order theory[c]	0.11853	0.63641	0.77755	1.4418	0.24487	0.65826	0.85872	1.7301
Present 3-D	0.11941	0.63834	0.76175	1.4316	0.24311	0.66377	0.85676	1.7014

[a] First-order theory – Reddy (1984)
[b] Third-order theory – Reddy and Liu (1985)
[c] Higher-order theory – Lim and Liew (1995)

Table 7. Comparison of frequency parameters $\lambda = \omega a\sqrt{\rho/E}$ for moderately thick fully clamped cylindrical shells of square planform computed based on three-dimensional theory and approximate theories ($a/R_m = 0.5$, $h/a = 0.1$)

Source of results	Symmetry classes and mode sequence number											
	SS-1	SS-2	SS-3	SA-1	SA-2	SA-3	AS-1	AS-2	AS-3	AA-1	AA-2	AA-3
First-order theory[a]	1.0766	3.1136	3.1604	1.9256	3.7041	3.7806	1.8752	3.7242	3.7754	2.6434	4.4398	5.0965
First-order theory[b]	1.0811	3.1221	3.1631	1.9310	3.7073	3.7860	1.8842	3.7343	3.7803	2.6497	4.4440	5.1036
Third-order theory[c]	1.0803	3.1298	3.1738	1.9369	3.7111	3.7959	1.8854	3.7351	3.7961	2.6595	4.4437	5.1385
Higher-order theory[d]	1.0822	3.1337	3.1746	1.9376	3.7110	3.7985	1.8888	3.7355	3.7962	2.6608	4.4441	5.1407
Present 3-D	1.0763	3.1073	3.1781	1.9382	3.7063	3.7817	1.8703	3.7214	3.7924	2.6499	4.4226	5.1104

[a] First-order theory with shear correction factor $\kappa = 5/6$ – Reddy (1984)
[b] First-order theory with shear correction factor $\kappa = 5/6$ – Lim (1994)
[c] Third-order theory – Reddy and Liu (1985)
[d] Higher-order theory – Lim and Liew (1995)

Table 8. Frequency parameters $\lambda = \omega a\sqrt{\rho/E}$ for a cantilever cylindrical shallow shell with $b/a = 1.0$

Curvature ratio a/R_m	Thickness ratio h/a	Symmetry classes and mode sequence number							
		S-1	S-2	S-3	S-4	A-1	A-2	A-3	A-4
0.1	0.01	0.015835	0.075039	0.085431	0.16678	0.026078	0.095562	0.19427	0.21795
	0.1	0.10487	0.61213	0.77336	1.4468	0.24472	0.66037	0.85854	1.7309
	0.2	0.20351	1.0724	1.3645	1.58613	0.44645	0.66151	1.45522	1.7726
	0.3	0.29392	1.3695	1.5883	1.7774	0.59892	0.66264	1.7721	1.8259
	0.4	0.37422	1.5492	1.5902	2.0656	0.66339	0.70897	1.7721	2.0579
	0.5	0.44408	1.5917	1.6551	2.2723	0.66443	0.78571	1.7718	2.2089
0.2	0.01	0.025455	0.080919	0.10646	0.17743	0.026948	0.10065	0.19471	0.22681
	0.1	0.10676	0.61562	0.77176	1.4449	0.24452	0.66079	0.85831	1.7274
	0.2	0.20427	1.0735	1.3612	1.5861	0.44597	0.66201	1.4542	1.7728
	0.3	0.29423	1.3697	1.5883	1.7735	0.59809	0.66342	1.7713	1.8257
	0.4	0.37425	1.5490	1.5902	2.0617	0.66350	0.70882	1.7721	2.0568
	0.5	0.44390	1.5917	1.6547	2.2684	0.66491	0.78527	1.7719	2.2077
0.3	0.01	0.035434	0.083294	0.12642	0.20159	0.02830	0.10837	0.19480	0.24031
	0.1	0.10986	0.62133	0.76917	1.4418	0.24418	0.66149	0.85793	1.7215
	0.2	0.20556	1.0754	1.3558	1.5862	0.44515	0.66286	1.4525	1.7731
	0.3	0.29475	1.3701	1.5883	1.7671	0.59673	0.66468	1.7699	1.8254
	0.4	0.37430	1.5487	1.5902	2.0550	0.66365	0.70860	1.7721	2.0550
	0.5	0.44360	1.5918	1.6539	2.2617	0.66571	0.78452	1.7721	2.2056
0.4	0.01	0.044583	0.086642	0.13735	0.23816	0.030056	0.11790	0.19451	0.25610
	0.1	0.11410	0.62902	0.76574	1.4373	0.24371	0.66248	0.85741	1.7129
	0.2	0.20739	1.0779	1.3483	1.5862	0.44401	0.66404	1.4502	1.7734
	0.3	0.29551	1.3707	1.5883	1.7580	0.59487	0.66642	1.7679	1.8249
	0.4	0.37439	1.5482	1.5902	2.0456	0.66381	0.70835	1.7721	2.0524
	0.5	0.44320	1.5918	1.6529	2.2523	0.66683	0.78348	1.7723	2.2026
0.5	0.01	0.052071	0.091858	0.14383	0.27308	0.032157	0.12841	0.19394	0.27155
	0.1	0.11941	0.63834	0.76175	1.4316	0.24311	0.66377	0.85676	1.7014
	0.2	0.20976	1.0812	1.3386	1.5862	0.44253	0.66557	1.4471	1.7739
	0.3	0.29652	1.3714	1.5882	1.7463	0.59254	0.66859	1.7652	1.8244
	0.4	0.37454	1.5476	1.5902	2.0334	0.66391	0.70813	1.7720	2.0490
	0.5	0.44271	1.5918	1.6516	2.2401	0.66825	0.78215	1.7726	2.1988

Table 9. Frequency parameters $\lambda = \omega a\sqrt{\rho/E}$ for a cantilever cylindrical shallow shell with b/a = 3.0

Curvature ratio a/R_m	Thickness ratio h/a	Symmetry classes and mode sequence number							
		S-1	S-2	S-3	S-4	A-1	A-2	A-3	A-4
0.1	0.01	0.0055510	0.033099	0.086430	0.15586	0.021451	0.067629	0.12301	0.1920
	0.1	0.034752	0.21589	0.60030	1.1642	0.20529	0.31485	0.64290	1.1550
	0.2	0.068739	0.42126	1.1456	1.5790	0.31482	0.38667	1.1973	1.4410
	0.3	0.10238	0.61287	1.5797	1.6144	0.31515	0.53790	1.4407	1.6469
	0.4	0.13549	0.78657	1.5805	2.0003	0.31545	0.65769	1.4415	1.9931
	0.5	0.16796	0.94056	1.5812	2.3113	0.31575	0.74784	1.4421	2.2511
0.2	0.01	0.0093500	0.054156	0.13292	0.20455	0.021746	0.069309	0.12818	0.20279
	0.1	0.035517	0.21999	0.60912	1.1761	0.20495	0.31533	0.64221	1.1542
	0.2	0.069066	0.42291	1.1490	1.5790	0.31470	0.38679	1.1953	1.4428
	0.3	0.10253	0.61356	1.5797	1.6157	0.31533	0.53763	1.4404	1.6467
	0.4	0.13551	0.78663	1.5805	2.0003	0.31575	0.65727	1.4422	1.9919
	0.5	0.16787	0.94014	1.5812	2.3104	0.31614	0.74733	1.4432	2.2496
0.3	0.01	0.013509	0.076686	0.17546	0.20466	0.022194	0.071898	0.13631	0.21939
	0.1	0.036774	0.22670	0.62361	1.1958	0.20440	0.31614	0.64110	1.1528
	0.2	0.069609	0.42570	1.1548	1.5790	0.31449	0.38700	1.1920	1.4456
	0.3	0.10275	0.61470	1.5797	1.6179	0.31563	0.53715	1.4398	1.6465
	0.4	0.13554	0.78672	1.5805	2.0003	0.31623	0.65655	1.4433	1.9899
	0.5	0.16773	0.93945	1.5812	2.3089	0.31680	0.74649	1.4450	2.2470
0.4	0.01	0.017813	0.098799	0.20277	0.20512	0.022752	0.075219	0.14690	0.24029
	0.1	0.038493	0.23590	0.64353	1.2230	0.20362	0.31725	0.63951	1.1509
	0.2	0.070380	0.42966	1.1630	1.5790	0.31416	0.38727	1.1874	1.4496
	0.3	0.10310	0.61632	1.5800	1.6210	0.31605	0.53652	1.4389	1.6463
	0.4	0.13560	0.78690	1.5805	2.0005	0.31692	0.65556	1.4448	1.9871
	0.5	0.16754	0.93852	1.5812	2.3069	0.31773	0.74526	1.4475	2.2434
0.5	0.01	0.022220	0.11944	0.20183	0.22051	0.023386	0.079161	0.15948	0.26403
	0.1	0.040638	0.24741	0.66855	1.2572	0.20262	0.31872	0.63750	1.1485
	0.2	0.071385	0.43482	1.1737	1.5790	0.31374	0.38769	1.1816	1.4546
	0.3	0.40355	0.61851	1.5797	1.6253	0.31659	0.53568	1.4376	1.6460
	0.4	0.13568	0.78717	1.5805	2.0008	0.31779	0.65427	1.4467	1.9835
	0.5	0.16731	0.93735	1.5812	2.3045	0.31893	0.74370	1.4507	2.2388

first-order shear deformable shell theory and the parabolic shear deformable shell theory proposed by Reddy and Liu (1985) and the higher-order theory of Lim and Liew (1995) are listed for comparison. It is observed that the solutions from both refined shell theories are comparable with the present three-dimensional elasticity solutions at the moderate thickness ratio of $h/a = 0.1$ with the three-dimensional elasticity solutions being generally slightly more conservative.

3.3 Parametric investigations

Tables 8 to 11 present the vibration frequencies for cylindrical shells with different boundary conditions. The frequency parameters presented in these tables are defined by Eq. (41) which are independent of the thickness h. For shells of constant width a, this parameter is directly proportional to the physical vibration frequency ω. Therefore, with this frequency parameter, the influence of various geometric parameters such as the relative shell thickness h/a and aspect ratio b/a upon the vibration frequency of the cylindrical shell can be directly investigated. To allow for the investigation on the effects of relative thickness ratio on the frequencies, shells with thickness ratio h/a ranging from 0.01 (a thin shell) to 0.5 (a thick shell) are considered. The shell shallowness ratio a/R_m is defined between 0.1 to 0.5 in the computations.

The frequency parameters for *CFFF* cylindrical shell with aspect ratios b/a of 1.0 and 3.0 are presented in Tables 8 and 9, respectively. It is observed that the lower vibration spectrum for both the thin and thick cantilever shells are dominated by the fundamental antisymmetric torsional mode (A-1). However, as the shell thickness increases, the symmetry bending mode (S-1) tends be the fundamental mode of vibration. In addition, it is found that the vibration frequencies for the cantilever shell tend to increase with the relative thickness ratio. This is because as the thickness increases, the bending and torsional stiffness of the shell also increase proportionally. However, it is noticed that for some modes (such as the A-3 mode for shells with $a/R_m = 0.3$ at thickness ratios h/a of 0.4 and 0.5), the increase in shell thickness does not have significant effects on the frequency value. Most of these modes (which will be demonstrated in the three-dimensional mode shape diagram), are found to be in-plane dominant shearing and stretching modes of vibration.

Comparing Tables 8 and 9 for cantilever shells of the same shallowness ratio (a/R_m) but with square ($b/a = 1$) and rectangular ($b/a = 3$) planforms, it is found that the fundamental frequencies for both the symmetry classes (S-1 and A-1) decrease with an increase in shell aspect ratios. The effects of aspect ratios upon the higher modes of vibration are more complex in nature. It is further deduced from Tables 8 and 9 that for relatively thin shallow shells

Table 10. Frequency parameters $\lambda = \omega a\sqrt{\rho/E}$ for simply-supported cylindrical square shells

Curvature ratio a/R_m	Thickness ratio h/a	Symmetry classes and mode sequence number											
		SS-1	SS-2	SS-3	SA-1	SA-2	SA-3	AS-1	AS-2	AS-3	AA-1	AA-2	AA-3
0.1	0.01	0.007820	0.29812	0.31138	0.16924	0.38840	0.51489	0.15039	0.39338	0.52681	0.24363	0.60048	0.61452
	0.1	0.57906	2.5856	2.5880	1.3822	1.9475	3.2479	1.3793	1.9483	3.2488	2.1207	3.8951	3.8967
	0.2	1.0605	2.7555	3.9932	1.9475	2.3294	4.3566	1.9483	2.3272	4.3555	3.3749	3.8951	3.8967
	0.3	1.4232	2.7556	4.5823	1.9476	2.9035	4.3566	1.9483	2.9014	4.3555	3.8950	3.8967	4.0412
	0.4	1.6867	2.7557	4.5054	1.9476	3.2555	4.3567	1.9483	3.2537	4.3552	3.8946	3.8967	4.4150
	0.5	1.8783	2.7557	4.3758	1.9475	3.4805	4.3567	1.9483	3.4789	4.3546	3.8938	3.8967	4.6392
0.2	0.01	0.11632	0.29782	0.34808	0.21862	0.39123	0.53990	0.15390	0.41086	0.52684	0.25818	0.61517	0.61586
	0.1	0.58316	2.5793	2.5912	1.3873	1.9451	3.2421	1.3757	1.9483	3.2476	2.1186	3.8902	3.8967
	0.2	1.0598	2.7561	3.9849	1.9452	2.3305	4.3565	1.9483	2.3212	4.3522	3.3703	3.8902	3.8967
	0.3	1.4202	2.7563	4.5793	1.9453	2.9030	4.3567	1.9483	2.8945	4.3520	3.8899	3.8967	4.0355
	0.4	1.6823	2.7565	4.5004	1.9453	3.2541	4.3568	1.9483	3.2461	4.3510	3.8886	3.8967	4.4084
	0.5	1.8728	2.7566	4.3658	1.9451	3.4785	4.3569	1.9483	3.4706	4.3483	3.8854	3.8967	4.6313
0.3	0.01	0.16125	0.29733	0.40192	0.28242	0.39597	0.57925	0.15964	0.43855	0.52686	0.28088	0.61624	0.64075
	0.1	0.58997	2.5687	2.5966	1.3957	1.9410	3.2324	1.36963	1.9483	3.2455	2.1150	3.8821	3.8967
	0.2	1.0587	2.7570	3.9710	1.9412	2.3324	4.3563	1.9483	2.3113	4.3466	3.3626	3.8822	3.8967
	0.3	1.4153	2.7575	4.5743	1.9414	2.9023	4.3567	1.9483	2.8829	4.3462	3.8814	3.8967	4.0259
	0.4	1.6751	2.7579	4.4920	1.9414	3.2519	4.3571	1.9483	3.2336	4.3440	3.8785	3.8967	4.3974
	0.5	1.8639	2.7582	4.3503	1.9410	3.4752	4.3572	1.9483	3.4569	4.3381	3.8715	3.8967	4.6183
0.4	0.01	0.20853	0.29667	0.46706	0.35300	0.40260	0.63028	0.16745	0.47479	0.52686	0.31010	0.61774	0.67416
	0.1	0.59946	2.5539	2.6041	1.4075	1.9353	3.2187	1.3611	1.9483	3.2427	2.1101	3.8706	3.8967
	0.2	1.0572	2.7581	3.9514	1.9356	2.3350	4.3560	1.9483	2.2973	4.3386	3.3518	3.8708	3.8967
	0.3	1.4086	2.7590	4.5673	1.9359	2.9014	4.3568	1.9483	2.8666	4.3381	3.8695	3.8967	4.0125
	0.4	1.6651	2.7598	4.4805	1.9360	3.2489	4.3574	1.9483	3.2160	4.3341	3.8643	3.8967	4.3821
	0.5	1.8516	2.7602	4.3303	1.9353	3.4707	4.3575	1.9483	3.4375	4.3239	3.8522	3.8967	4.6003
0.5	0.01	0.25694	0.29586	0.53952	0.41116	0.42712	0.69045	0.17718	0.51796	0.52680	0.34440	0.61967	0.71502
	0.1	0.61156	2.5346	2.6137	1.4226	1.9279	3.2011	1.3502	1.9483	3.2392	2.1038	3.8557	3.8967
	0.2	1.0555	2.7596	3.9242	1.9283	2.3385	4.3556	1.9483	2.2791	4.3283	3.3378	3.8559	3.8967
	0.3	1.4002	2.7609	4.5584	1.9288	2.9002	4.3567	1.9483	2.8454	4.3274	3.8539	3.8967	3.9953
	0.4	1.6525	2.7621	4.4661	1.9289	3.2451	4.3577	1.9483	3.1931	4.3214	3.8460	3.8967	4.3624
	0.5	1.8361	2.7626	4.3067	1.9278	3.4650	4.3579	1.9483	3.4126	4.3060	3.8276	3.8967	4.5774

($h/a \leq 0.1$), higher frequencies are observed at large shallowness ratio a/R_m. As the shell thickness increases, the variations of the frequency parameters with respect to the shallowness ratio are less predictable. It is due mainly to the presence of several in-plane vibration modes which are not affected by the shallowness ratio of the shells. The vibration characteristics of *CFFF* shells can be further clarified by considering the vibration mode shapes.

Figures 2 and 3 show the three-dimensional displacement contour plot and deformed mode shapes of cantilevered shallow shells with square ($b/a = 1$) and rectangular ($b/a = 3$) planforms, respectively. The shallowness ratio, for this case, is chosen at $a/R_m = 0.5$ and the thickness ratio is assumed to be $h/a = 0.2$. The modes are arranged in ascending sequence number. The first four modes, based on appearance, can be classified as spanwise bending, chordwise bending, spanwise torsional and chordwise torsional modes, respectively for the square and rectangular shells. The higher modes of vibration are more complex and involve strong couplings between the flexural and torsional motions.

The thickness independent frequency parameter λ, for *SSSS* and *CCCC* shells of square planform are presented in Tables 10 and 11, respectively. The numerical results are arranged into four symmetry classes with reference to the x_1x_2- and x_2x_3-planes. These are the doubly symmetric modes (SS), the symmetric-antisymmetric modes (SA), the antisymmetric-symmetric modes (AS) and the doubly antisymmetric modes (AA). The analyses are carried out for shells with shallowness ratio a/R_m ranges from 0.1 to 0.5 and thickness ratio h/a from 0.01 (a thin shell) to 0.5 (a thick shell). The variations of the vibration frequencies with respect to the thickness ratio h/a, for the *SSSS* and *CCCC* shells follow the same pattern as the *CFFF* shell. As the relative thickness increases, the frequency value for the fundamental mode of the *SSSS* and *CCCC* shells also increases. The fundamental mode for these shell configurations exhibits predominantly out-of-plane vibration motion. This mode is most susceptible to the increase in shell stiffness following the increase in the relative thickness. From Tables 10 and 11, it is found that the vibration frequencies for most of the modes increase with respect to the thickness ratios. However, the vibration frequencies of certain modes which are dominated by in-plane motion tend to remain constant as the shell thickness varies. This is observed for the SA-2, AS-2, AA-2 and AA-3 modes of the *SSSS* shell. Such in-plane dominant vibration modes are less significant in *CCCC* shells as shown in Table 11. It is observed that for the *CCCC* shells, most modes increase in value as the shell thickness increases.

Three-dimensional mode shapes for the *SSSS* and *CCCC* cylindrical shells of square planform are presented in

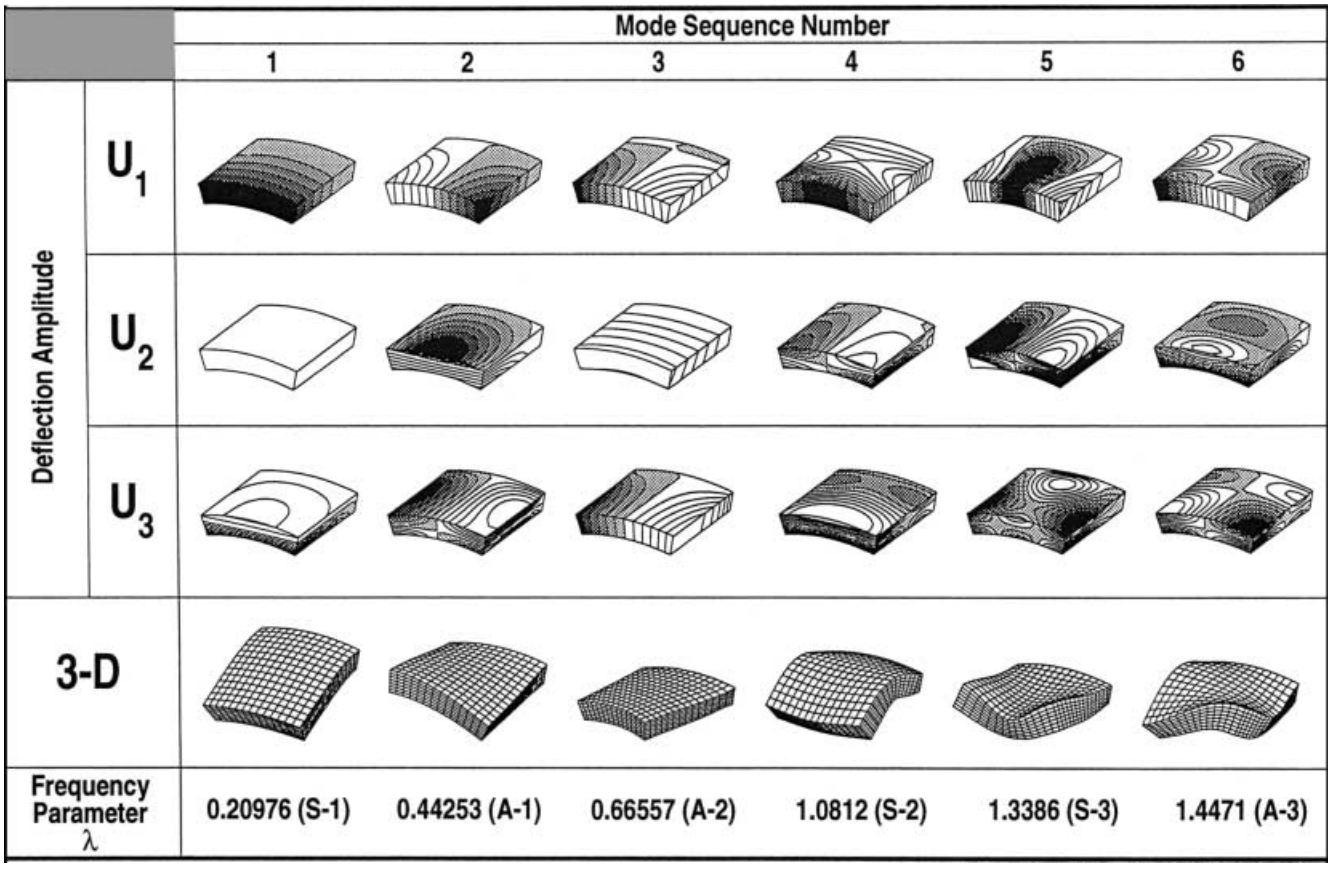

Fig. 2. Mode shapes and frequency parameters $\lambda = \omega a\sqrt{\rho/E}$ for the cantilevered (*CFFF*) circular cylindrical square shell panel ($b/a = 1$, a/R_m 0.5 and $h/a = 0.2$)

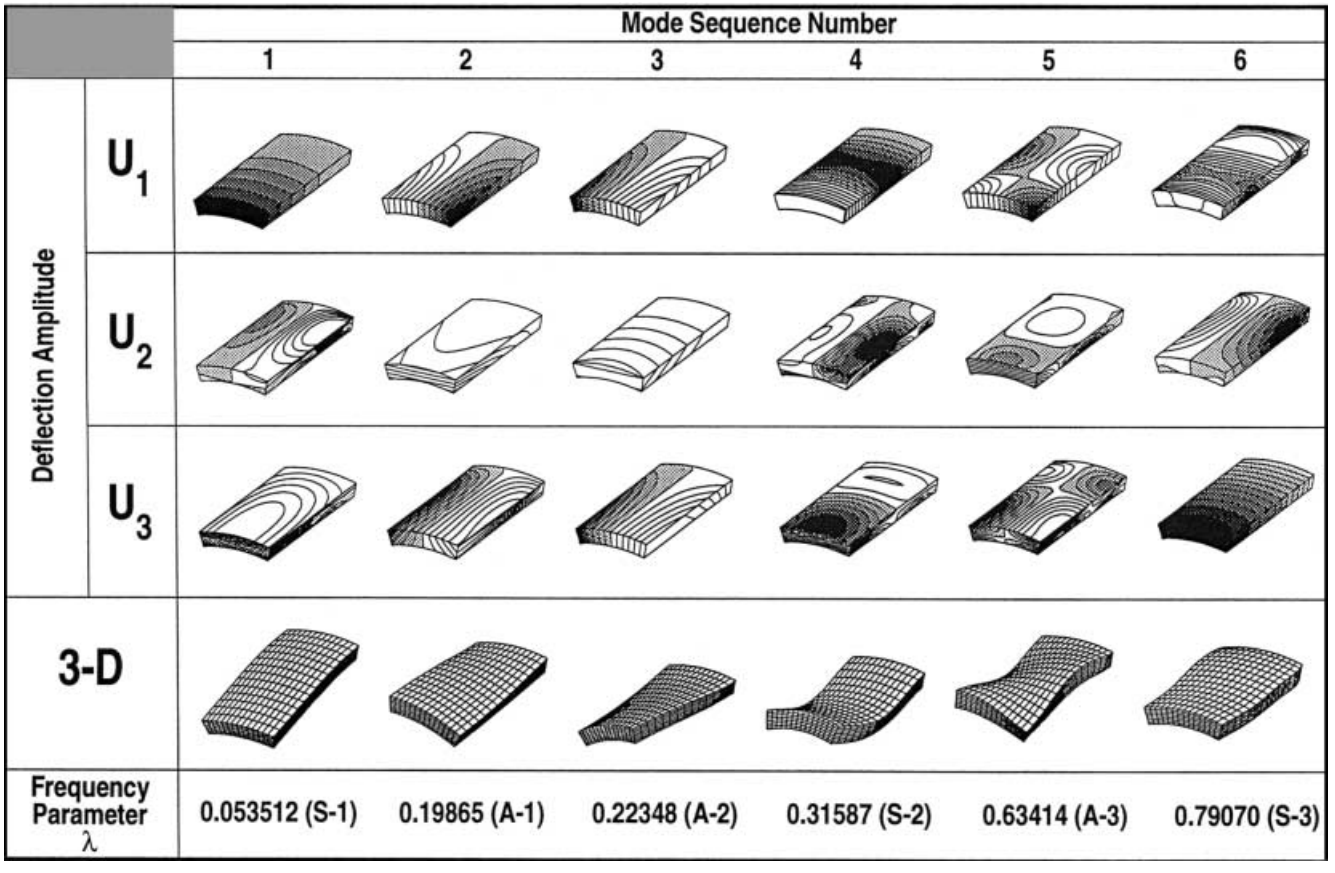

Fig. 3. Mode shapes and frequency parameters $\lambda = \omega a\sqrt{\rho/E}$ for the cantilevered (*CFFF*) circular cylindrical rectangular shell panel ($b/a = 2$, a/R_m 0.5 and $h/a = 0.2$)

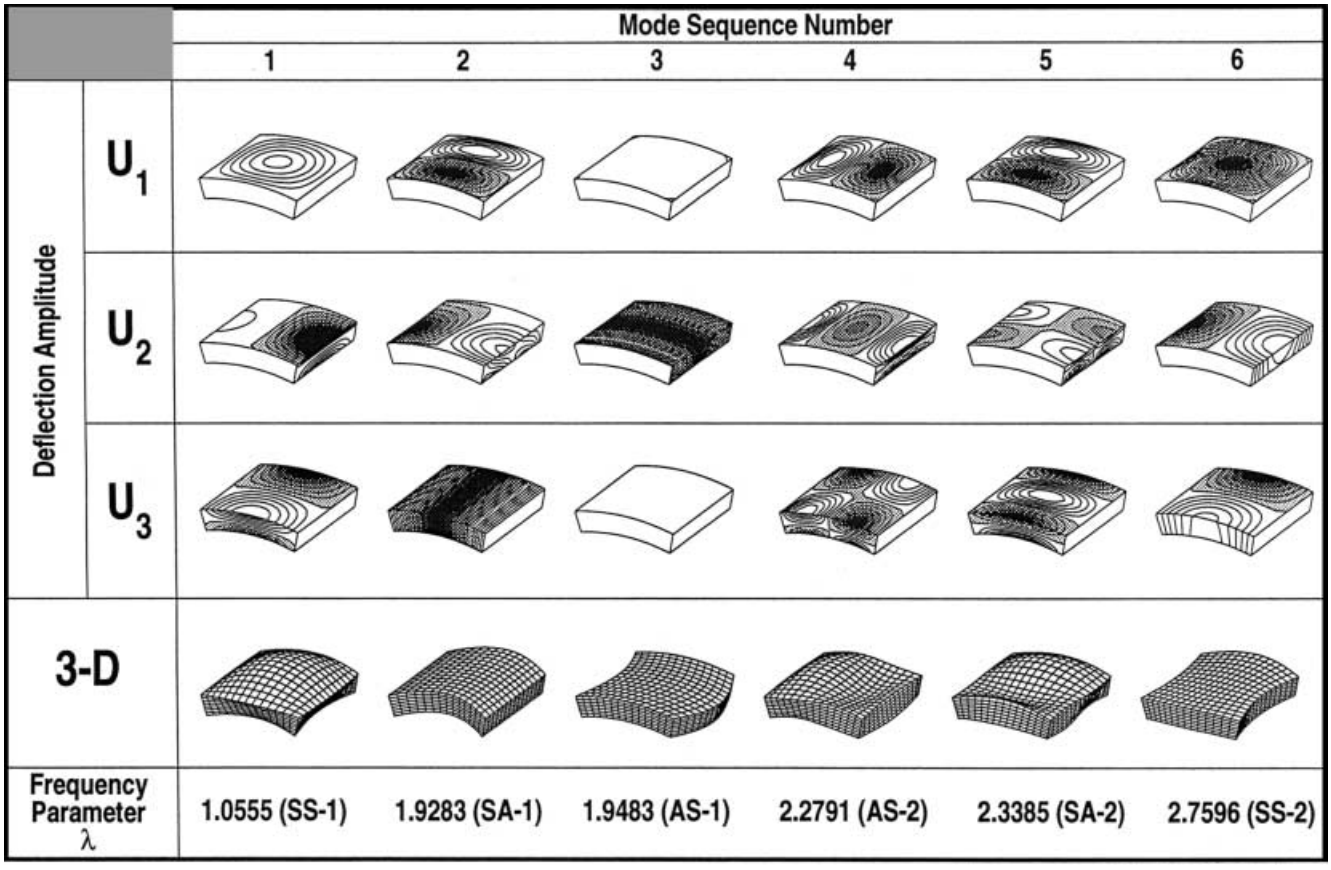

Fig. 4. Mode shapes and frequency parameters $\lambda = \omega a\sqrt{\rho/E}$ shell panel ($b/a = 1$, a/R_m 0.5 and $h/a = 0.2$) for the simply-supported (*SSSS*) circular cylindrical square

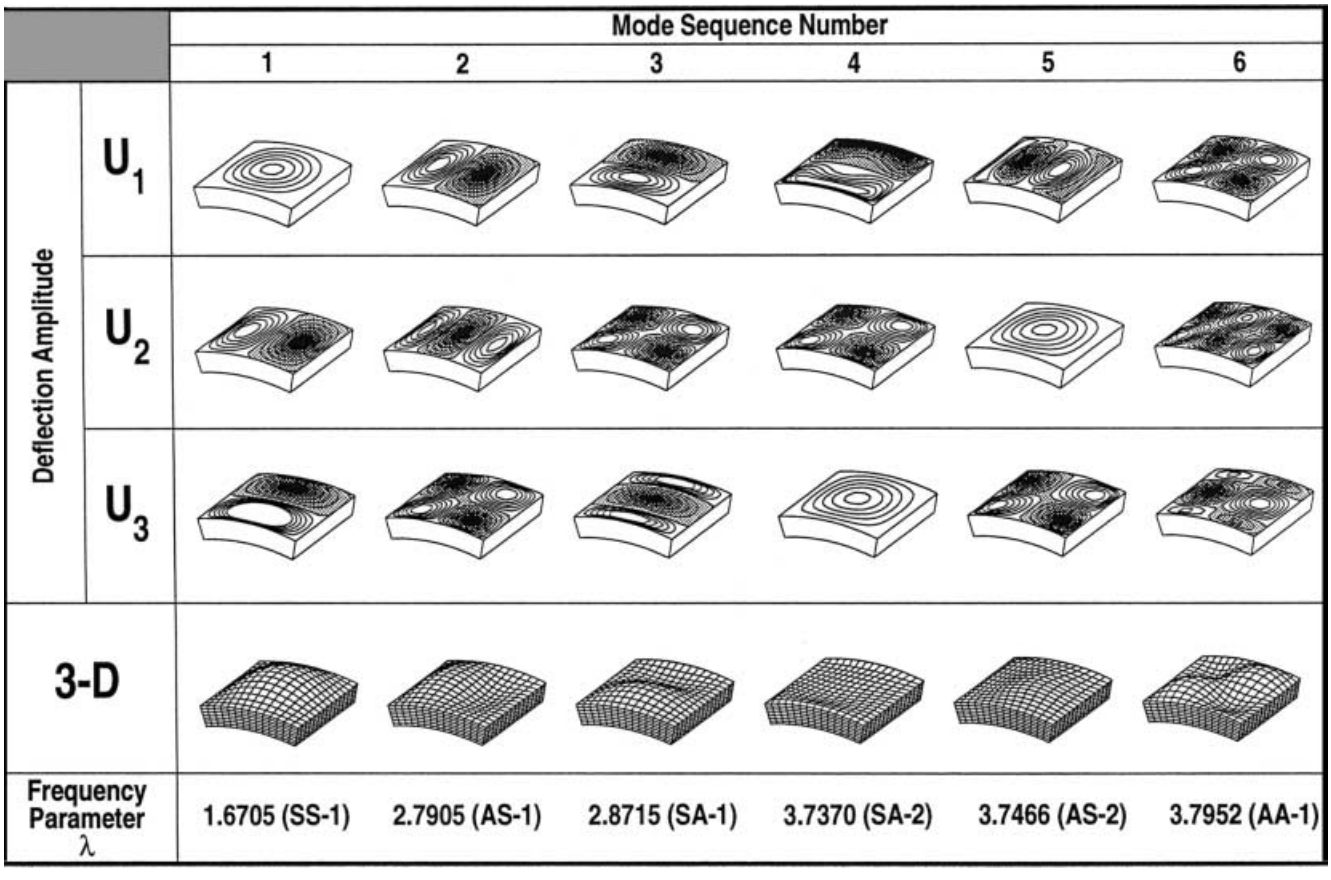

Fig. 5. Mode shapes and frequency parameters $\lambda = \omega a\sqrt{\rho/E}$ shell panel ($b/a = 1$, a/R_m 0.5 and $h/a = 0.2$) for the fully clamped (*CCCC*) circular cylindrical square

Table 11. Frequency parameters $\lambda = \omega a\sqrt{\rho/E}$ for fully clamped cylindrical square shells

Curvature ratio a/R_m	Thickness ratio h/a	Symmetry classes and mode sequence number											
		SS-1	SS-2	SS-3	SA-1	SA-2	SA-3	AS-1	AS-2	AS-3	AA-1	AA-2	AA-3
0.1	0.01	0.14047	0.40385	0.41004	0.24023	0.50376	0.64248	0.22720	0.50522	0.64160	0.33474	0.73589	0.73911
	0.1	0.99818	3.1396	3.1716	1.8976	3.7383	3.8041	1.9012	3.7417	3.7974	2.6635	4.4407	5.1655
	0.2	1.6330	4.3799	4.4416	2.8524	3.7470	5.2058	2.8564	3.7505	5.1982	3.8378	4.4423	5.4572
	0.3	1.9899	4.8994	4.9726	3.2909	3.7523	5.7771	3.2938	3.7567	5.7657	4.3449	4.4473	5.4546
	0.4	2.1946	5.1761	5.2509	3.5157	3.7550	6.0210	3.5162	3.7608	6.0137	4.4403	4.6162	5.4428
	0.5	2.3188	5.3488	5.4206	3.6449	3.7559	5.4581	3.6412	3.7637	5.4639	4.4418	4.7726	5.4201
0.2	0.01	0.20489	0.41033	0.44068	0.28631	0.51034	0.66330	0.23760	0.52211	0.64139	0.35267	0.73910	0.75122
	0.1	1.0083	3.1388	3.1693	1.9027	3.7347	3.8008	1.8973	3.7392	3.7969	2.6618	4.4385	5.1613
	0.2	1.6380	4.3771	4.4382	2.8549	3.7458	5.1986	2.8490	3.7506	5.1956	3.8330	4.4416	5.4538
	0.3	1.9938	4.8964	4.9686	3.2927	3.7512	5.7679	3.2831	3.7590	5.7614	4.3298	4.4563	5.4507
	0.4	2.1981	5.1728	5.2461	3.5173	3.7540	6.0103	3.5010	3.7655	6.0097	4.4286	4.6210	5.4377
	0.5	2.3224	5.3439	5.4134	3.6463	3.7549	5.4597	3.6194	3.7716	5.4741	4.43231	4.7735	5.4128
0.3	0.01	0.27338	0.42549	0.48731	0.34786	0.52234	0.69656	0.25383	0.54900	0.64110	0.38039	0.74195	0.77348
	0.1	1.0250	3.1344	3.1683	1.9112	3.7285	3.7958	1.8909	3.7350	3.7959	2.6589	4.4348	5.1521
	0.2	1.6465	4.3710	4.4339	2.8590	3.7437	5.1865	2.8368	3.7506	5.1912	3.8251	4.4403	5.4479
	0.3	2.0001	4.8901	4.9632	3.2957	3.7493	5.7526	3.2657	3.7623	5.7544	4.3086	4.4673	5.4443
	0.4	2.2040	5.1657	5.2396	3.5198	3.7523	5.9914	2.4773	3.7719	6.0026	4.4106	4.6275	5.4293
	0.5	2.3284	5.3329	5.4043	3.6486	3.7532	5.4622	3.5880	3.7800	5.4906	4.4170	4.7747	5.4008
0.4	0.01	0.32729	0.46003	0.54503	0.41358	0.54265	0.74048	0.27464	0.58428	0.64083	0.41548	0.74617	0.80367
	0.1	1.0478	3.1240	3.1713	1.9231	3.7192	3.7892	1.8819	3.7292	3.7944	2.6550	4.4295	5.1356
	0.2	1.6582	4.3596	4.4307	2.8648	3.7408	5.1696	2.8199	3.7504	5.1851	3.8142	4.4383	5.4367
	0.3	2.0090	4.8787	4.9581	3.2998	3.7467	5.7312	3.2420	3.7661	5.7448	4.2836	4.4780	5.4353
	0.4	2.2122	5.1528	5.2334	3.5233	3.7499	5.9635	3.4464	3.7785	5.9918	4.3877	4.6343	5.4176
	0.5	2.3367	5.3125	5.3968	3.6518	3.7510	5.4658	3.5497	3.7867	505128	4.3966	4.7753	5.3846
0.5	0.01	0.35710	0.52051	0.60912	0.47138	0.57866	0.79308	0.29880	0.62610	0.64079	0.45550	0.75228	0.84079
	0.1	1.0763	3.1074	3.1781	1.9382	3.7063	3.7817	1.8703	3.7214	3.7924	2.6499	4.4227	5.1104
	0.2	1.6705	4.3299	4.4285	2.8715	3.7370	5.1361	2.7905	3.7466	501745	3.7952	4.4353	5.4268
	0.3	2.0203	4.8605	4.9548	3.3051	3.7434	5.7037	3.2125	3.7699	5.7327	4.2556	4.4874	5.4236
	0.4	2.2227	5.1322	5.2292	3.5277	3.7469	5.9267	3.4095	3.7843	5.9773	4.3609	4.6403	5.4026
	0.5	2.3438	5.2640	5.3900	3.6541	3.7476	5.4699	3.4994	3.7862	5.5369	4.3711	4.7706	5.3601

Figs. 4 and 5. The shell configurations chosen are those with shallowness ratio of $a/R_m = 0.5$ and relative thickness ratio h/a of 0.2. For the freely supported conditions, the edges are allowed to deform normally but not tangentially to the plane containing the edge. It is noticed that for both the *SSSS* and *CCCC* shells, the first six vibration modes are mostly transverse bending modes. Only certain modes, particularly for the *SSSS* shells, are dominated by in-plane vibratory motions.

4
Conclusion

A three-dimensional elasticity solution for the free vibration problem of thick cylindrical shell panels of rectangular planform has been presented. The governing eigenvalue equation for the continuum was derived from the three-dimensional elasticity theory and employing the Ritz minimization procedure. Converged results obtained compared very well with corresponding finite element simulation results using MSC/NASTRAN. Further favorable comparisons were made with existing experimental and numerical results in the literature. For shells of high thickness-to-width ratios, it is believed that the present method provides more accurate results than classical and refined shell theories. Results for a wide range of thick cylindrical shell panels of various boundary conditions and linear parameters have been presented and a detailed discussion into parametric investigations has been provided. Displacement mode shapes in three-dimension were plotted for visualization enhancement and thus better understanding of the vibratory motions.

References

Armenakas AE, Gazis DC, Herrmann G (1969) Free vibrations of circular cylindrical shells, Pergamon Press, Oxford

Cheung YK, Li WY, Tham LG (1989) Free vibration analysis of singly curved shell by spline finite strip method. J. Sound and Vibr. 128: 411–422

Deb Nath JM (1969) Dynamics of rectangular curved plates, Ph.D. Thesis, Univ. of Southampton, UK

Hung KC, Liew KM, Lim MK (1995) Free vibration of cantilevered cylinders: effects of cross-sections and cavities. Acta Mechanica 113: 37–52

Leissa AW (1973) Vibration of shells, NASA SP-288, US Government Printing Office, Washington DC

Leissa AW, Lee JK, Wang AJ (1981) Vibrations of cantilevered shallow cylindrical shells of rectangular planform. J. Sound and Vibr. 78: 311–328

Liew KM, Hung KC (1995) Three-dimensional vibratory characteristics of solid cylinders and some remarks on simplified beam theories. Int. J. Solids Struct. 32: 3499–3513

Liew KM, Hung KC, Lim MK (1995a) Free vibration studies on stree free three-dimensional elastic solids. Trans. ASME J. Appl. Mech. 62: 159–165

Liew KM, Hung KC, Lim MK (1995b) Vibration of stress-free hollow cylinders of arbitrary cross section. Trans. ASME J. Appl. Mech. 62: 718–724

Liew KM, Lim CW, Kitipornchai S (1997) Vibration of shallow shells: a review with bibliography. Trans. ASME Appl. Mech. Review 58: 431–444

Lim CW, Liew KM (1994) A *pb*-2 Ritz formulation for flexural vibration of shallow cylindrical shells of rectangular planform. J. Sound and Vibr. 173(3): 343–375

Lim CW, Liew KM (1995) A higher-order theory for vibration of shear deformable cylindrical shallow shells. Int. J. Mech. Sci. 37(3): 277–295

Love AEH (1888) The small free vibrations and deformations of thin elastic shells. Phil. Trans. Royal Society (London), ser. A 179: 491–549

Love AEH (1927) Treatise on the mathematical theory for thin shell, NASA Technical Report R-24

Olson MD, Lindberg GM (1969) Vibration analysis of cantilevered curved plates using a new cylindrical shell finite element. Proc. Of the 2nd Conf. On Matrix Methods in Structural Mech., Wright-Patterson Air Force Base, Ohio AFFDL-TR-69-150, pp. 247–270

Olson MD, Lindberg GM (1971) Dynamic analysis of shallow shell with a doubly-curved triangular finite element. J. Sound and Vibr. 19: 299–318

Qatu MS (1989) Free Vibration and static analysis of laminated composite shallow shells, Ph.D. Thesis, The Ohio State University, US

Reddy JN (1984) Exact solutions of moderately thick laminated shells. Trans. ASCE J. Eng. Mech. 110(5): 794–809

Reddy JN, Liu CF (1985) A higher-order shear deformation theory of laminated elastic shell. Int. J. Eng. Sci. 23: 319–330

So J (1993) Three-dimensional vibration analysis of elastic bodies of revolution, Ph.D. Thesis, The Ohio State University, US

Soldatos KP, Hadjigeorgiou VP (1990) Three-dimensional solution of the free vibration problem of homogeneous isotropic cylindrical shells and panels. J. Sound and Vibr. 137(3): 369–384

Walker KP (1978) Vibrations of cambered helicoidal fan blades. J. Sound and Vibr. 59: 35–57

Webster JJ (1968) Free vibration of rectangular curved panels. Int. J. Mech. Sci. 10: 571–582